Estimation of three-dimensional error covariance statistics for an ocean assimilation system

Ocean Applications Technical Note No. 30

M.J. Martin, M.J. Bell and A. Hines

November 2002

Produced by the Met Office
Met Office London Road Bracknell Berkshire RG12 2SZ United Kingdom
Tel +44 (0)1344 856465 Fax: +44 (0)1344 854499
E-mail: matthew.martin@metoffice.com www.metoffice.com

Estimation of three-dimensional error covariance statistics for an ocean assimilation system

Ocean Applications Technical Note No. 30

M.J. Martin, M.J. Bell and A. Hines

November 2002

Summary

A new set of estimates of observation and model error covariance statistics has been constructed for the Forecasting Ocean Asssimilation Model (FOAM) system. These statistics have been calculated from three years of collocated observation and model forecast data using a method based on Hollingsworth and Lönnberg (1986). The calculations represent each univariate component of the forecast error covariance as the sum of two second-order autoregressive (SOAR) functions with different correlation scales which are intended to represent errors in the ocean mesoscale and at the atmospheric synoptic scale. The statistics are calculated for appropriate sub-domains to allow the statistics to vary geographically (i.e. be inhomogeneous).

The data used in the calculations are sea surface height (SSH) data from satellite altimeters, surface temperature (SST) data from in-situ and satellite platforms and in-situ temperature profile data. The model forecasts in this paper are from a 20 level configuration of the FOAM system for the Atlantic and Arctic which has a grid spacing of 40km.

For the SST and SSH it is found that the mesoscale variances have a marked maximum in the Gulf Stream region and that the mesoscale correlation scales have relatively little geographical variation with typical values of 40-60km. The synoptic scale errors for SST and SSH have much longer correlation scales (typically 300km for SSH and 500km for SST) and both the variance and correlation scales vary relatively little geographically.

Vertical correlation scales have been estimated using temperature profile data for both error components. The mesoscale length scales appear to be significantly longer than those for the synoptic scale. To estimate from the statistics how the SSH data should be projected in the vertical, the temperature profile data has also been used to calculate isopycnal displacement statistics as a function of depth. These show a maximum displacement variance at the thermocline depth with a decrease in displacement above and below.

1. Introduction

A major international effort to demonstrate the viability and value of operational ocean forecasting is planned for the period 2003-2005 (GODAE, 2002). This period coincides with improvements to the ocean observing system such as the implementation of the Argo array of profiling floats (Argo Science Team, 1998) and the operational dissemination of altimeter data from the Jason-1 and Envisat satellites. To make the most of these and other observations, the schemes which assimilate them into ocean circulation models need to be developed so as to produce more accurate initial conditions for forecasts.

Most of the methods used for assimilating data require some knowledge of the errors in the system. These observation and model forecast error covariances need to be known *a priori* for methods such as Optimal Interpolation (OI) or 3D-Var in which they are usually kept constant (Daley, 1991). For more advanced methods such as the ensemble Kalman filter, the error covariances are implicitly evolved with the analyses, although some initial estimate is required (Evensen, 1997). The error covariance matrices are not known exactly and could not be specified exactly even if they were known due to their size ($\sim 10^7 \times 10^7$ for a 1° resolution global ocean model) so they have to be approximated in some manner.

There are various methods in the literature for estimating the error covariance matrices. The method of Hollingsworth and Lönnberg (1986, hereafter referred to as HL) can be used to estimate both the forecast and observation error covariances. Here, collocated observation and model forecast values are used to form the error statistics. The NMC method (Parish and Derber, 1992) compares forecasts with different lead times which are valid at the same time and uses many realisations to estimate the forecast error statistics. It is usually used to produce statistics for a range of horizontal and vertical wave numbers using spectral techniques. The specification of the model forecast error covariance matrix is crucial to the effectiveness of any data assimilation scheme as it determines how the observation increments are spread onto the model field.

The true model forecast error covariance matrix will be spatially inhomogeneous in the horizontal and will contain energy in many different scales. The method of HL introduced above is usually used to estimate statistics which vary in the horizontal but only one correlation scale is calculated. Conversely, the NMC method is usually used to estimate multi-scale error statistics, homogeneous in the horizontal, for a wide range of spectral scales. In this work, a method whereby the different oceanic signals present in the observations can be extracted will be sought using a method based on that of HL so that the resulting error statistics will be both spatially inhomogeneous and multi-scale.

Section 2 describes the assumptions and methods used to estimate error statistics. The data and model used in the calculations are described in section 3. The methods used assume separability between horizontal and vertical errors. The estimates of horizontal statistics are described in section 4 and the vertical statistics in section 5. The shortcomings of the methods used and the results, together with some suggestions for improvement are discussed in section 6. Section 7 presents a concluding summary. Estimates of error statistics for salinity over the north Atlantic and Arctic are briefly described in Appendix A and global statistics for SST are shown in Appendix B.

2. Assumptions and method used to calculate error covariance statistics

The forecast error covariance matrix P^f is very large. A standard method for representing P^f specifies the variances V from its diagonal elements and correlation functions f which give smooth approximations to the off-diagonal elements, thus reducing the dimensions of the problem. Writing the forecast error covariance matrix as described gives

$$P^f_{(ij)} = \sqrt{V_i V_j} f_{(ij)}(x_i, x_j), \tag{2.1}$$

where $P^f_{(ij)}$ is the forecast error covariance at point i, j and x is the variable for which the covariance is to be determined. This covariance can be written as the sum of K standard functions (such as Gaussian or SOAR functions), each with their own scale, that is

$$P^f_{(ij)} = \sum_{k=1}^{K} \sqrt{V_i^k V_j^k} g^k_{(ij)}(x_i, x_j). \tag{2.2}$$

An important requirement of correlation functions is that they be positive definite so that the resulting covariance matrix is positive definite. Any linear combination of positive definite functions with nonnegative constants is also a positive definite function (Weber and Talkner, 1993).

The method of HL uses collocated observation values, denoted by y_i at point i, and model forecast values (of the same quantity) denoted by x_i^f to estimate the variances and correlation scales. This is valid if the observation errors are uncorrelated and the forecast and observation errors are not cross-correlated. If these assumptions hold then

$$\begin{aligned} &< (x_i^f - y_i)(x_j^f - y_j) > \\ &= < [(x_i^f - x_i^t) + (x_i^t - y_i)][(x_j^f - x_j^t) + (x_j^t - y_j)] > \\ &= < (x_i^f - x_i^t)(x_j^f - x_j^t) > + 2 < (x_i^f - x_i^t)(x_j^t - y_j) > + < (x_i^t - y_i)(x_j^t - y_j) > \\ &= < (x_i^f - x_i^t)(x_j^f - x_j^t) >, \end{aligned} \tag{2.3}$$

where $< . >$ indicates an ensemble mean, i and j are observation locations ($i \neq j$), superscript f denotes the forecast value and superscript t denotes the "truth" (see Lorenc, 1986 for a definition). This shows that the ensemble mean covariance of the forecast errors at two observation locations can be calculated from the differences between observation and forecast values. The forecast error covariance can therefore be calculated directly from the data as a function of separation between points. Assuming that the error covariance data is smoothly varying with separation, a predetermined function can then be fitted to the covariance data and the correlation scale and the forecast error variance can be estimated. Extrapolating these covariances to zero separation then gives estimates of the forecast error variances (HL).

Assuming that forecast and observation errors are not cross-correlated, the ensemble mean variances between collocated observation and forecast values can be re-expressed as the sum of the forecast and observation error as

$$\begin{aligned} <(x_i^f - y_i)^2> &= <(x_i^f - x_i^t + x_i^t - y_i)^2> \\ &= <(x_i^f - x_i^t)^2> + <(y_i - x_i^t)^2>. \end{aligned} \tag{2.4}$$

The observation error variance can therefore be estimated (at least in principle) by calculating the difference between the forecast error covariance at zero separation and the forecast minus observation variance.

The calculations described above need to be performed for a given area with sufficient observations to obtain statistically meaningful results. The number of observations available therefore limits the resolution of the grid on which the statistics can be estimated. The amount of data available will depend on both the type of data and the period over which the calculations are performed. So for a given period over which observations are available, the spatial resolution of the statistics which can be calculated will be different for each data type. The statistics are assumed to be homogeneous in each grid box over which they have been calculated. Anisotropic statistics could in principle be calculated in each grid box, but only isotropic values have been obtained in this work.

Correlation functions have to be specified to represent the error covariance data. The model forecast is likely to contain errors on many different horizontal and vertical scales and it is important to use knowledge about the dynamics of the ocean to specify the type of functions used to represent these scales. Also, the correlation scales which are used should be appropriate for the particular application. For instance, different scales are important for short range forecasts (5-10 days) and longer range applications such as seasonal or climate prediction. For these longer time scale applications, where the model grid is often of much coarser resolution, processes which occur on small spatial scales can be viewed as noise in the system and may be included in the errors of representativity of the observations. For short range, high resolution forecasts, it is important to include these small scale features in the forecast error statistics.

The number of different correlation scales that are to be extracted from the data depends on the type of application. In short range ocean forecasting it is thought that there are two main sources of model forecast error. The first arises from errors in the forcing of the model by atmospheric fields such as the wind or freshwater forcing, or in the response of the model to such large scale forcing. Errors in the wind forcing are likely to occur on horizontal scales similar to those for synoptic weather systems in mid-latitudes (of order a few 100kms) with fairly small correlation with errors in the deep ocean. Errors in the freshwater fluxes applied to the ocean model may have smaller time and horizontal scales as they will mainly affect errors in the mixed layer. These type of errors are expected to be small compared with those for the large scale wind forcing and so are ignored here although might be treated in future work. Errors which occur on scales similar to those of atmospheric synoptic scale systems are called "synoptic scale" errors in this work.

The second source of forecast error arises from errors in the internal dynamics of the model. These internal errors are likely to be associated with the baroclinic modes of the ocean and hence consist of several horizontal and vertical scales. At present, the resolution in FOAM is such that many of the higher baroclinic modes are not resolved. Only the first baroclinic mode is dealt with in this report although the work could be extended to include some of the higher modes. The first baroclinic mode is likely to have horizontal errors on scales of a few tens of kilometres with large vertical scales. These types of errors are termed "mesoscale" errors in this report.

Two second order auto-regressive (SOAR) functions are used in this work to represent the two types of model forecast error described above. Univariate error covariance correlation functions are written as

$$P(r) = V_{mes}(1 + r/L_{mes})e^{-r/L_{mes}} + V_{syn}(1 + r/L_{syn})e^{-r/L_{syn}}, \qquad (2.5)$$

where r is the separation distance between two points, subscript *mes* indicates the mesoscale component, subscript *syn* indicates the synoptic scale component, V is the variance and L is the correlation length scale. A set of separation distances r_i are defined and the covariance data is put into bins which surround each distance (the separation distances are shown in figure 3). The function P is then fitted to the covariance data z_i using a descent algorithm which minimises the χ^2 value which is a measure of the goodness of fit of the function to the data and is given by

$$\chi^2 = \sum_i \frac{1}{\sigma_i^2}[z_i - P(r_i)]^2, \qquad (2.6)$$

where σ is some weighting factor which indicates how well the data should be fitted at different points. The algorithm which is used to minimise this value is the steepest descent method which makes changes to initial estimates of the parameters to be estimated, namely the length scales and variances, based on the gradients of χ^2 with respect to each parameter normalised by the norm of the gradients. The nonlinearity of the function in equation (2.5) means that the final values of the parameters have some dependence on their initial estimates. An example of the initial values of the parameters used for the calculation of SSH covariance data is $L^0_{mes} = 50km$, $L^0_{syn} = 150km$, $V^0_{mes} = 50cm^2$ and $V^0_{syn} = 10cm^2$.

3. Data used in calculations

3.1 Model fields

The operational FOAM system currently includes two model configurations. A global model with 1° horizontal resolution was implemented in 1997. A north Atlantic and Arctic model with 40km (1/3°) grid spacing, which takes its boundary conditions from the global model was implemented in April 2001. Both these models have a vertical grid with 20 levels which range in resolution from 10m in the upper ocean to about 500m at depth. The model dynamics and parameterisations are very similar to those used in the ocean component of the HadCM3 climate simulations (Gordon *et al.* 2000). The models are forced by 6-hourly wind stress, evaporation-minus-precipitation, heat flux and radiation fields derived from the Met Office's operational NWP system. For more information about the model see Bell *et al.* (2000).

The statistics in this paper were calculated using one day forecasts from an integration of the north Atlantic and Arctic model which ran for 3 years between 1997 and 1999. The initial conditions were produced from a model-only integration of the same model and boundary conditions were taken from a run of the global model which assimilated SST and temperature profile data. The main integration assimilated quality controlled SSH, SST and temperature profile data using an implementation of the analysis correction scheme described by Bell *et al.* (2000).

3.2 Observations

Observation and model forecast values have been output at observation positions from the 3 year run of the FOAM 1/3° system described above. Only those observations which passed the quality control contribute to the statistics. The number of these observations in two degree boxes from the three years of integration is approximately 1.1×10^6 SST and 9.4×10^6 SSH observations. There are enough of both of these observation types to enable root mean square (RMS) values to be calculated on a 2° grid although the SST results are likely to be noisier than those for SSH as there are less of these observations. Calculations of covariances have been performed on a 10° grid for these data types to ensure there are enough observations to produce realistic statistics. The number of temperature profile observations is significantly smaller, the total number of observations (counting those for each depth separately) being approximately 1.4×10^5. These observations have been used to compute error covariances only as basin averages although RMS values have been estimated on a 10° grid for comparison with SST data.

4. Horizontal error statistics

Values for the total RMS errors in 2° grid boxes are shown for SSH and SST data in figures 1(a) and (b) respectively. For both data types, errors are largest in the Gulf Stream region, reaching maxima of about 40cm for SSH and about 4K for SST data. This is to be expected as this area has a large amount of variability. The errors are probably larger than they might have been (at 300km) because the length scales used in the assimilation were quite large so that the small scale eddies in the Gulf Stream would not have been accurately represented.

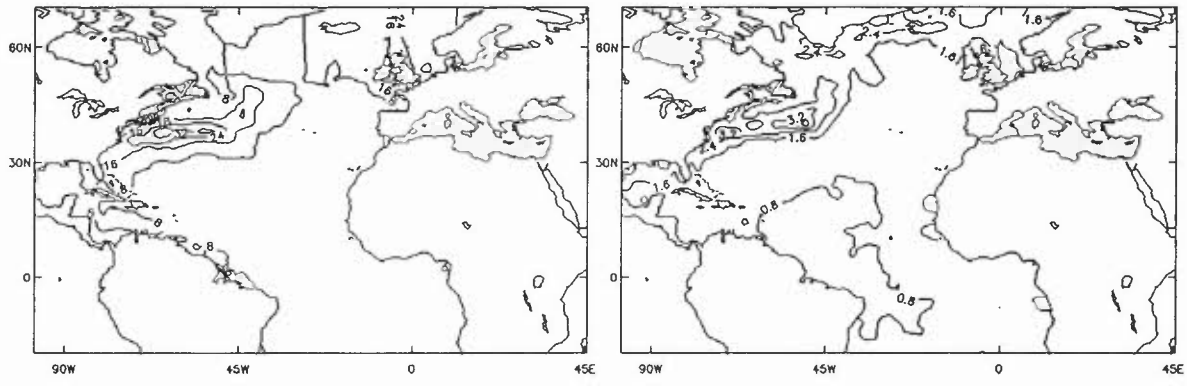

Figure 1: RMS values of (observation - forecast) for (a) SSH (cm) and (b) SST (K).

The RMS patterns (on a 10° grid) for the temperature profiles are fairly similar to those of SST in the upper levels with values of 0.5-1K in most of the region, increasing to about 2.6K in the Gulf Stream region as shown in figure 2. There is a slight increase in the errors with depth down to about 150m, especially in the equatorial region where errors in the model's density gradients in the thermocline are likely to cause larger errors. Below 150m, the errors decrease except in the Gulf Stream region where they remain relatively constant down to about 600m.

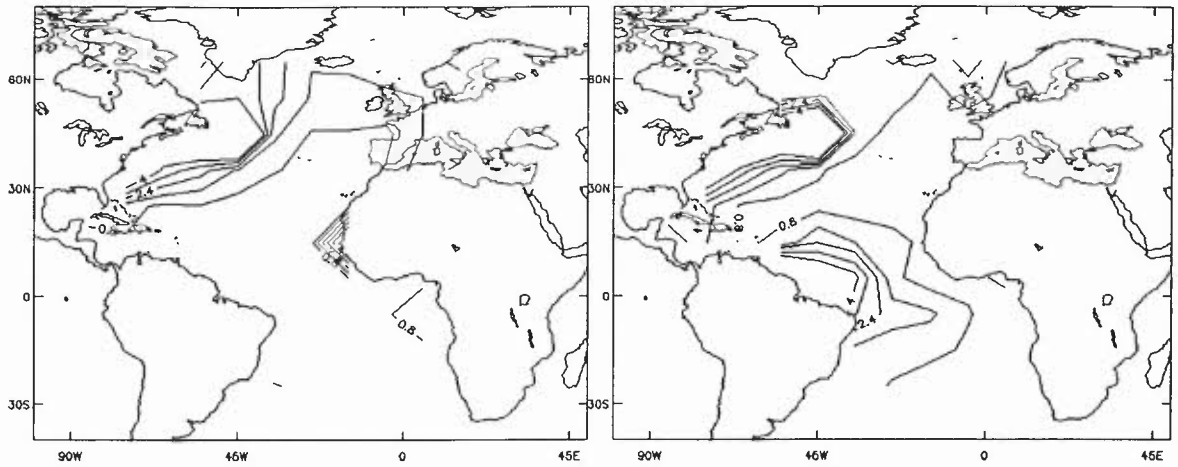

Figure 2: RMS values of (observation - forecast) for temperature profile data (K) at (a) the surface and (b) 150m.

4.1 Sea surface height

Estimates of the forecast error statistics for SSH have been computed using the method described in section 2 with a 10° grid. Two examples of the fit to the data are shown in figure 3. The first example is at a grid box in the centre of the north Atlantic, away from the western boundary current, and two scales can clearly be distinguished. The dotted line shows the mesoscale errors which have a length scale of about 40km. The synoptic scale errors are shown by the dashed line and have a length scale of about 560km. These scales are fairly typical of boxes over the whole of the region. The ratio of the variances is more variable. In the second of the examples, the mesoscale errors completely dominate the signal because it is in a region of high eddy activity in the Gulf Stream. The total forecast variance is over 300cm^2 compared to about 30cm^2 for the first example. Now only one scale is extracted from the fit to the data and this scale is about 40km, similar to values in most of the region for the mesoscale. In this example, there is a slight negative covariance at about 200km separation which is not captured by the function fit to the data. It would be possible to use a different function to include negative covariances but this is not attempted here as these negative lobes are of small magnitude and only occur in one or two grid boxes.

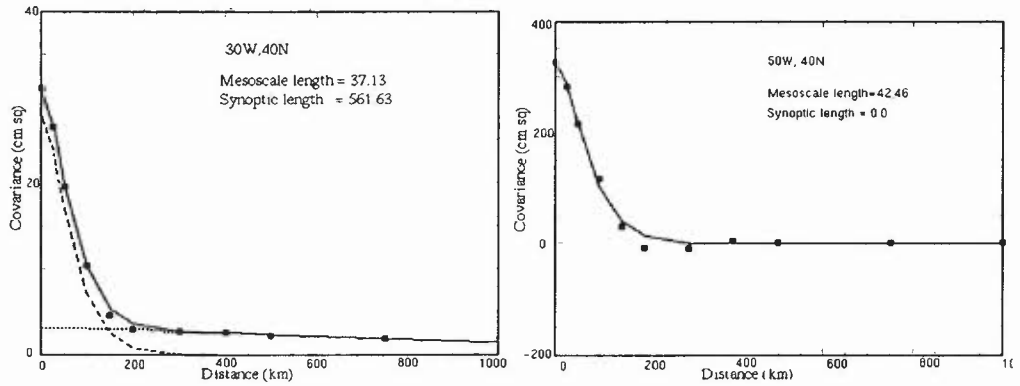

Figure 3: Examples of fits to the SSH covariance data (cm^2) using two SOAR functions (a) at 30W, 40N and (b) at 50W, 40N. Shown are the covariance data (circles), the mesoscale errors (dotted line), the synoptic scale errors (dashed line) and the total errors (solid line).

To use the results of this analysis in the assimilation, it is desirable to process the fields in appropriate ways. The total SSH RMS errors on a 2° grid shown in figure 1(a) have been combined with the results of the analysis of the mesoscale forecast error variances on a 10° grid so that the regions of high mesoscale variance can be more accurately defined. This was accomplished by interpolating both the synoptic scale and observation variances onto a 2° grid and subtracting them from the total RMS field. The results are shown in figure 4(a). The Gulf Stream region is clearly defined and has much larger mesoscale variances than the rest of the north Atlantic. There are regions to the northeast and northwest of the region with large variances. These are areas where the model does not perform well due to the shallow depth of the ocean. The synoptic scale error variances are not shown here because they are fairly constant over the whole of the region and an average value is therefore used of about 9cm^2. This is much smaller than the mesoscale variances over most of the region.

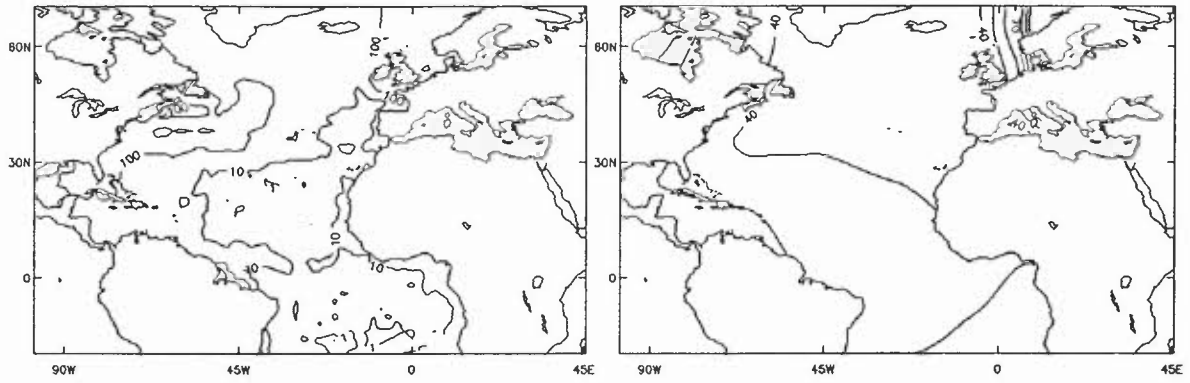

Figure 4: SSH mesoscale forecast error (a) variance (cm^2) and (b) correlation length scale (km).

The mesoscale correlation scales have been smoothed and interpolated onto a 2° grid and are shown in figure 4(b). The smoothing was applied by replacing the value at each gridpoint with the average value over the 3x3 box centred on that point. The resulting scales are fairly constant over the north Atlantic at about 40km although they do increase slightly in the Gulf of Mexico. There are also larger scales in the southeast of the region. This might be associated with the flow which enters the region through the southern boundary which comes from the 1° model which inherently has larger scales. It could also be due to the fact that the scales are isotropic in these calculations whereas flow near the equator is known to have longer zonal scales than meridional scales. The synoptic length scales have been averaged over the whole region as they are fairly constant at about 400km.

Observation error variances have been calculated from the difference between the total RMS errors and the total forecast error variance and are shown in figure 5. These errors are of similar magnitude to the synoptic scale forecast error variances at about 10cm^2 over most of the region. They include both the actual errors in the observations and the errors incurred by trying to use observations valid at a single point to infer information about fields on a model grid with a 30km resolution.

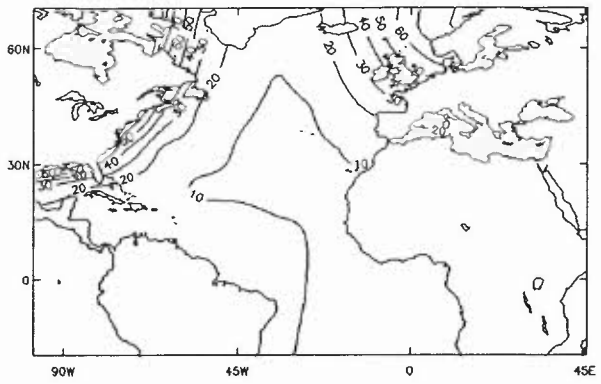

Figure 5: SSH observation error variance (cm^2).

4.2 Sea surface temperature

The error statistics for SST have been calculated in the same way as for SSH and show qualitatively similar results. The mesoscale forecast variances are again much larger in the Gulf Stream region, as can be seen in figure 6(a), with maximum values of about $12K^2$. The synoptic scale variances are fairly constant with an average value of about $0.2K^2$ and are not shown here. The mesoscale length scales are about 50-70km over most of the region and increase towards the Gulf of Mexico as can be seen in figure 6(b). There now seems to be some decrease in the scales towards the equator which is the opposite to those obtained with SSH data. The synoptic length scales have an average value of about 500km. The observation error variances are slightly larger than for the synoptic scale errors, with values varying from about $0.1K^2$ up to $2K^2$. This is shown in figure 7.

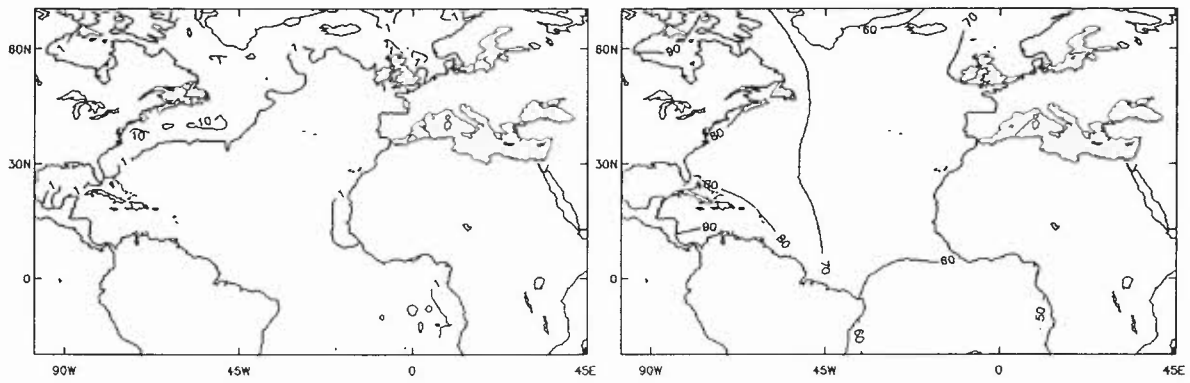

Figure 6: SST mesoscale forecast error (a) variance (K^2) and (b) correlation length scale (km).

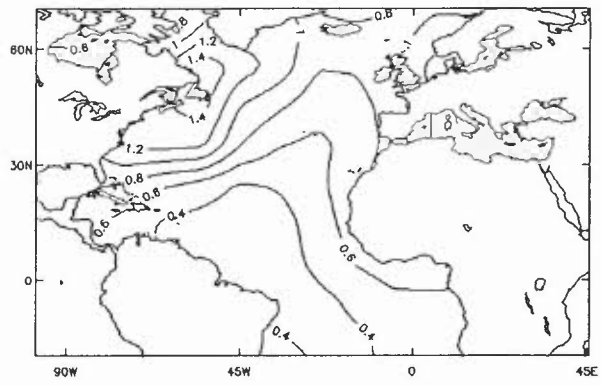

Figure 7: SST observation error variance (K^2).

4.3 Temperature profiles

A basin wide average of error variances and correlation scales for temperature profile data was calculated as a function of depth. The mesoscale and synoptic scale forecast error variances are shown in figures 8(a) and (b) respectively. These show that both components are maximum at about 50m depth and decrease with depth. The mesoscale has larger errors with a maximum of about $1.8K^2$. The synoptic scale error variances decrease more rapidly with depth and are less than $0.2K^2$ by about 200m depth.

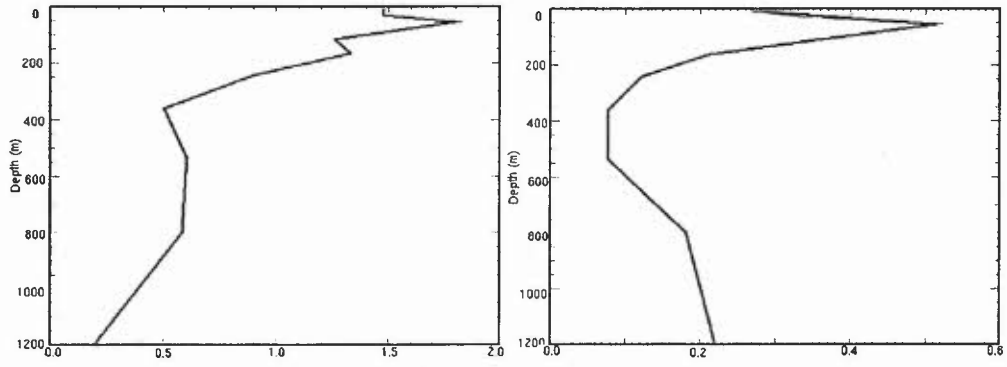

Figure 8: Temperature profile forecast error variance (K^2) (a) mesoscale and (b) synoptic scale.

Figures 9(a) and (b) show the forecast error correlation length scales for the mesoscale and synoptic scale components respectively. The mesoscale length scales are fairly constant between about 40 and 50km throughout the top 1000m of the ocean although they do increase slightly between 200 and 400m depth. The synoptic scales are about 700km at the surface, increasing to over 1000km at 50m depth and then decreasing to about 500km. At a number of depths, these synoptic correlation scales are 500km which was the initial estimate for the function fitting algorithm. The final χ^2 value was small at these depths ($0.01477K^2$ at 1200m for example) which indicates that the function did fit the data well and that the minimisation was insensitive to the synoptic correlation scale.

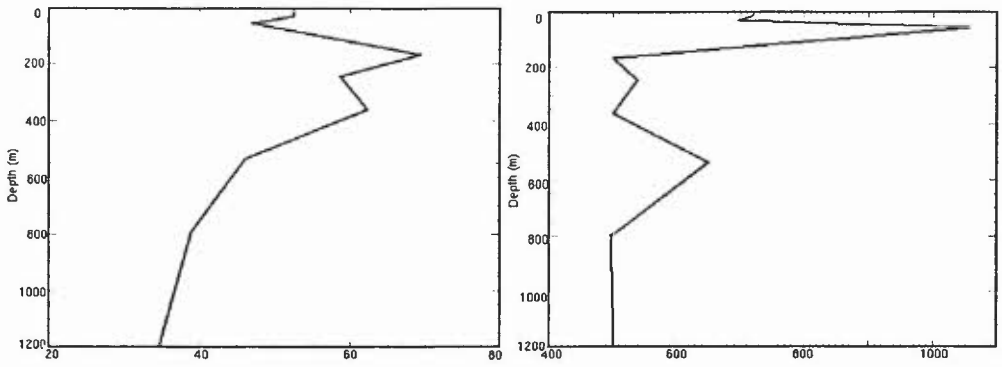

Figure 9: Temperature profile forecast error correlation length scales (km) (a) mesoscale and (b) synoptic scale.

The observation error variance for temperature profile data was estimated by averaging the total RMS data over the whole north Atlantic and subtracting the sum of the mesoscale and synoptic scale variances shown in figure 8. The results are shown in figure 10 and show that the observation error variance is generally small compared to the total forecast variance. The slight negative value at about 700m depth indicates that this estimate of the variance might not be very accurate.

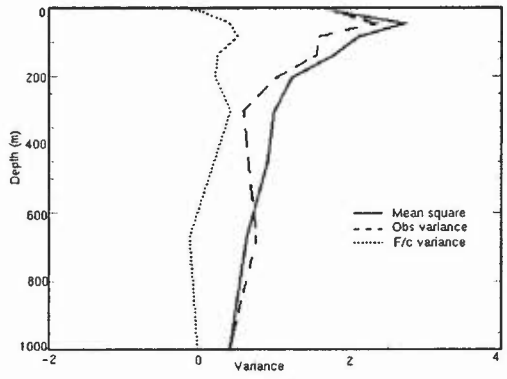

Figure 10: Temperature profile total mean square errors (solid line), total forecast error variance (dashed line) and observation error variance (dotted line) (K^2).

5. Vertical error statistics

5.1 Vertical isopycnal displacement variances

One of the aims of this work is to test the validity of the Cooper & Haines (1996) scheme. To do this, the temperature profile data was used to calculate statistics of isopycnal displacements. The first stage of the calculation was to convert the model and observed temperature values to density values. This was done by using the Levitus salinity data set so that for each temperature value, a salinity value was interpolated to the correct position for the same time of year.

For each pair of model and observed density profiles, a functional was minimised which described the amount the model density profile would have to be displaced in order for it to

equal the observed density at each depth, allowing for some additional synoptic scale error in the "horizontal" placement of the profile. This is done by minimising the following functional with respect to ρ,

$$\mathcal{J}(\rho) = (\rho_k^o - \rho)B_{syn}^{-1}(\rho_k^o - \rho) + (z_k - h^m(\rho))B_v^{-1}(z_k - h^m(\rho)), \qquad (5.1)$$

where ρ_k^o is the density on the observed profile at level z_k, $h^m(\rho)$ is the depth of the density value on the model profile and B_{syn} and B_v specify the weightings for the horizontal and vertical displacement errors respectively. In other words, for density ρ_k^o on the observed profile at level z_k, find the density ρ on the model profile which minimises the difference in height between level z_k and the height of ρ on the model profile, allowing for errors in the placement of ρ_k^m in the horizontal, as shown schematically in figure 11. Then the isopycnal displacement is given by $(z_k - h^m(\rho_{\min}))$ where $\rho_{\min}$ is the minimum of the cost function given in equation (5.1).

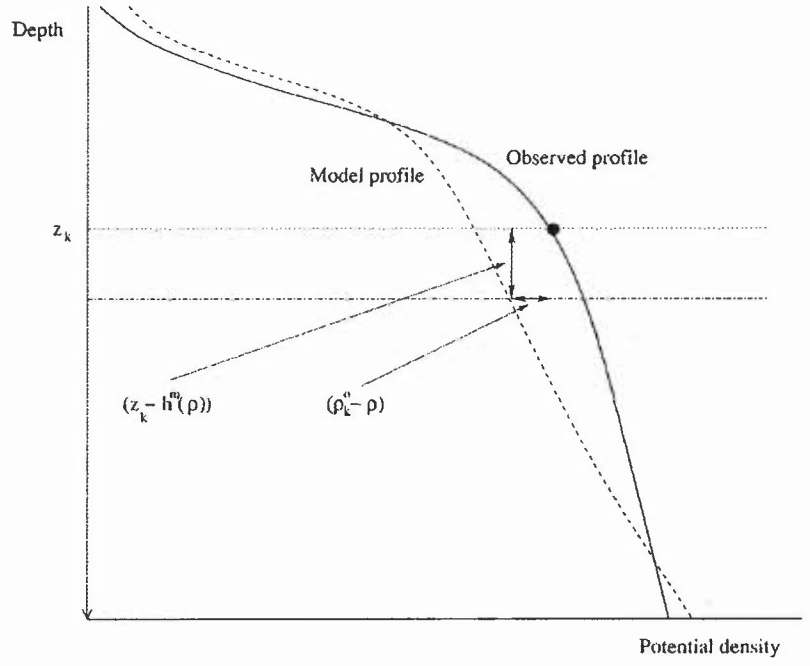

Figure 11: Schematic of the calculations for isopycnal displacement.

The minimum of the cost function depends strongly on the specification of the weights B_{syn} and B_v. The horizontal errors in the placement of model density profiles should depend on the synoptic scale horizontal error variances, as only those parts of the errors in the vertical which are due to the mesoscale should be extracted. These have already been calculated for temperature as averages over the whole basin as a function of depth and are shown in figure 8(b). These are therefore used for B_{syn}, after converting to density variances using the thermal expansion coefficient.

The vertical weight should be some estimate of the variance in the vertical displacement of isopycnals. This poses a problem as this is similar to the quantity we are trying to deduce. We

therefore parameterise this quantity by the value $D = (SSH\ RMS)/(\rho_1 - \rho_K)$, the SSH RMS divided by the difference between the density at the top and the density at the bottom of the profile. This is an estimate of the lifting and lowering implied by the SSH RMS. These RMSs have already been calculated, as shown in figure 1(a) and are used on the 10° grid. So B_v is constant with depth but varies horizontally.

The functional in equation (5.1) was minimised for each pair of model and observed profiles at each depth down to 1000m. The results were then split into three regions according to the SSH RMS. These are shown in figure 12, along with the average depth of the thermocline in the different regions and the isopycnal displacement variance implied by the Cooper & Haines scheme which is given by D^2. For all three regions, the general picture is that the isopycnal displacements are maximum in the region of the thermocline and decrease above and below this depth. The displacements also increase near the surface which is likely to be due to large errors in the mixed layer.

In regions of small SSH RMS where the eddy activity is fairly small, the Cooper & Haines scheme seems to overestimate the isopycnal displacement. As the SSH RMS increases, the value implied by the Cooper & Haines scheme explains less and less of the isopycnal displacement below the top 150m. This is a surprising result as errors in regions of high SSH RMS are expected to be regions with large vertical scales because of the vertical coherence of eddies.

These results seem to compare reasonably well with those of Faucher *et al.* (2002), where isopycnal EOFs are calculated as a function of depth over the north and tropical Atlantic from a set of historical hydrographic data. In the Gulf Stream, they find that the isopycnal displacement has a maximum at mid-depths for the first EOF, which corresponds to the maximum variance at the thermocline depth in this work. They find that the first EOF is vertically homogeneous in regions outside the Gulf Stream, indicating the lifting/lowering should be as implied by the Cooper & Haines scheme. This result is different from the results shown here although the rest of the signal might be explained by the higher EOFs. The use of large amounts of historical data in their work means that they are able to give spatially varying estimates of the EOFs. In this work, values for only three regions can be computed due to the number of data, but the results should be more relevant to the FOAM system than using the historical data. Also, it is possible to use the results in a way which enables spatial and temporal variability by letting the displacement of the isopycnals depend on the model's thermocline depth, as indicated by the results.

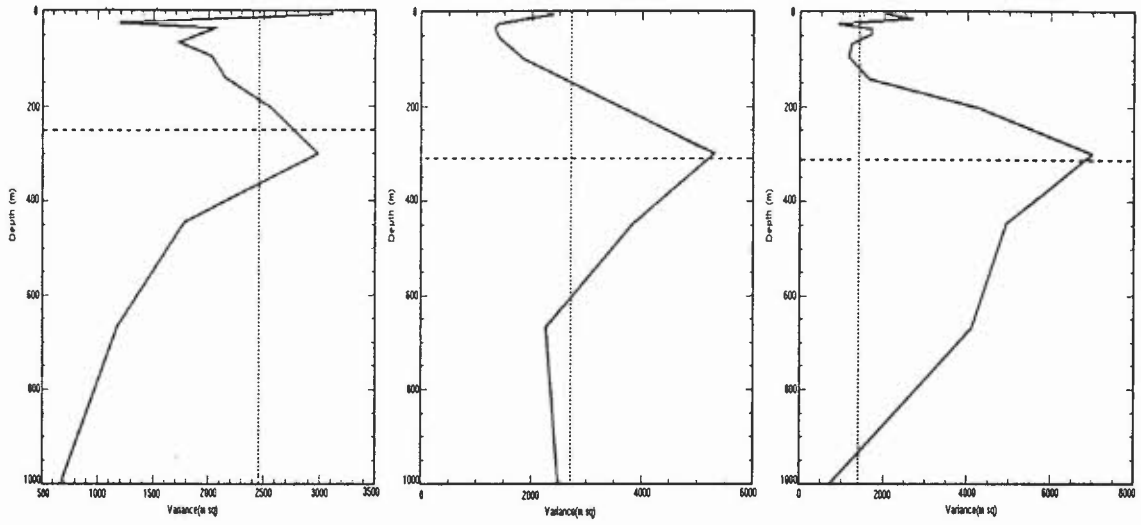

Figure 12: Isopycnal displacement variance (m^2) (solid line) with depth for regions dependent on SSH RMS (a) SSH RMS < 10cm (b) 10cm < SSH RMS < 20cm (c) 20cm < SSH RMS. Also shown is the average thermocline depth (dashed line) and the isopycnal displacement variance implied by the Cooper & Haines scheme (dotted line).

5.2 Temperature profiles

With the two component error covariance matrices described in section 3.1, two components of the vertical correlation scales are required for the temperature data so that the mesoscale and synoptic scale errors are put into the correct part of the vertical signal. A method for calculating the synoptic part of these errors using the temperature profile errors is shown schematically in figure 13. For each depth on a profile, correlations are calculated between the value at this depth and the values at all the different depths on another profile. These correlations are then binned in terms of the distance between the two profiles. This is done for all the pairs of profiles available which have a separation of less than 1000km. So for each depth and separation, the correlations with other depth levels are available. Two SOAR functions are then fitted to the data, one to estimate correlations above this depth and one below it so that two length scales are obtained for each depth and for each separation. These results are then averaged at each depth for separations between 200 and 1000km so that none of the mesoscale signal will be included.

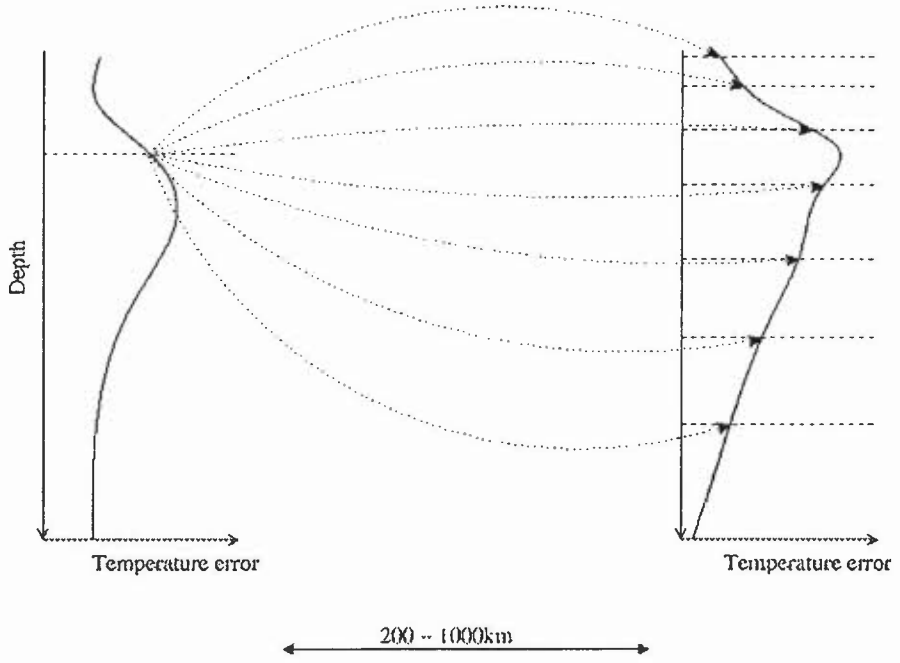

Figure 13: Schematic of the calculations for vertical error statistics for synoptic scale temperature.

The results of these calculations are shown in figure 14. This shows the vertical correlation scales for the synoptic component of the temperature error as a function of depth. For each depth the two scales are shown together with the average. The results show that, on average, the vertical correlation scales for the synoptic component are about 70m. This value increases at about 100m depth to a maximum of about 160m for those points below this depth.

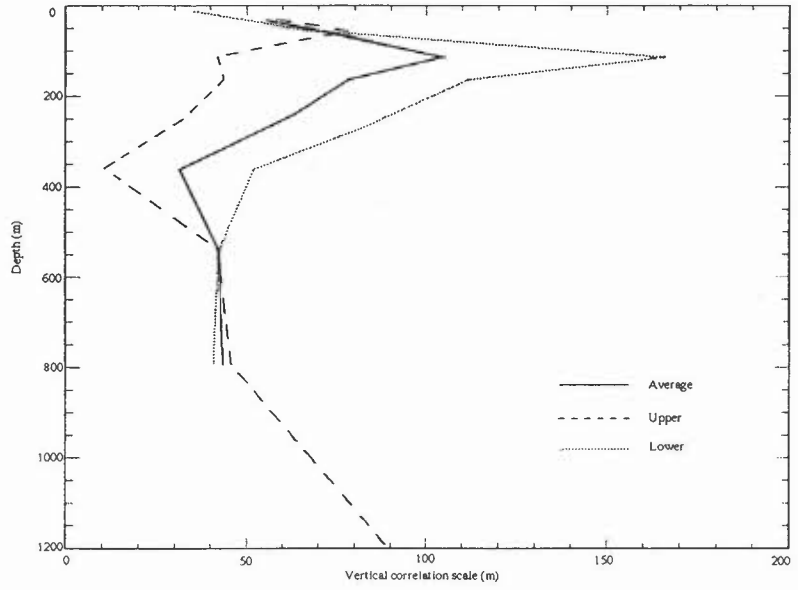

Figure 14: Vertical error correlation scales for temperature profile data for the synoptic scale. Shown are correlations above (dashed) and below (dotted) each depth along with the average of the two (solid).

Calculations have also been performed which attempt to estimate the vertical correlation scales for the mesoscale component of the temperature errors by using the covariance statistics obtained during the isopycnal displacement calculations. The synoptic scales have been taken out by allowing the profile to have horizontal errors so these statistics give information about how the density is correlated in the vertical for the mesoscale component. Since climatological salinity values were used to calculate both the forecast and observed density profiles, the statistics will also be relevant to the vertical temperature displacements. It is assumed here that the vertical displacement covariance statistics will be similar to the vertical covariances of temperature errors.

Two SOAR functions were fitted to the isopycnal displacement covariance statistics for each of the three regions distinguished by the SSH RMS. One of these functions estimated the correlation length scale above and one below each depth for the three regions. The results of these calculations are shown in figure 15. The initial estimate for the fitting routine to calculate the length scales was set to be 150m. For the region with small SSH RMS especially, the data was not very coherent at some depths and so the fitting routine failed to estimate the length scales and returned with the initial estimate. In the two regions where the SSH RMS is larger, the length scales vary between about 70m and 190m which is a fairly large variation. Overall, the average value for the vertical correlation scale for the mesoscale is about 120m.

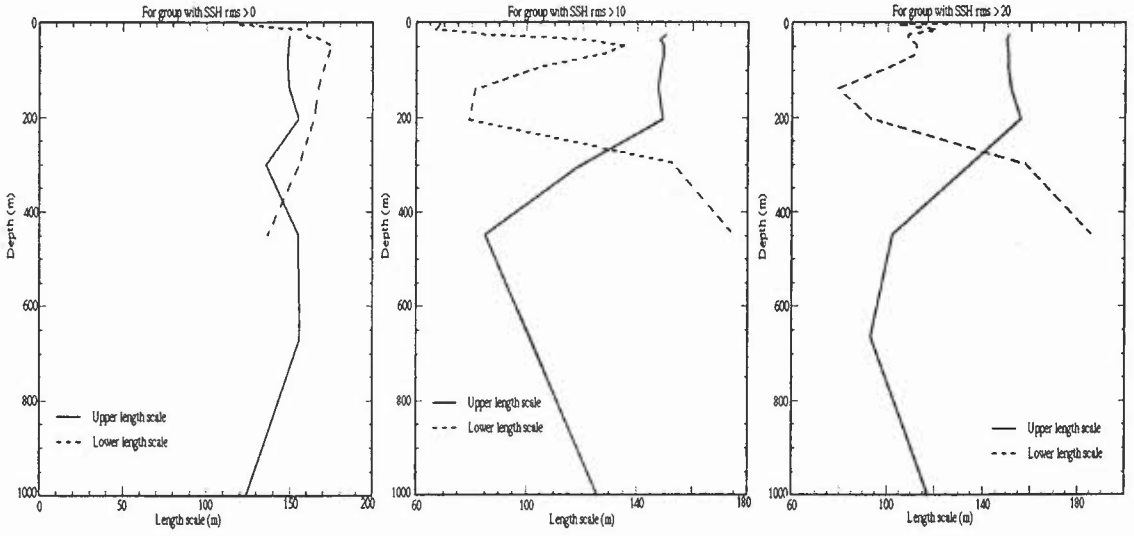

Figure 15: Vertical error correlation scales for temperature profile data for the mesoscale for regions dependent on SSH RMS (a) SSH RMS < 10cm (b) 10cm < SSH RMS < 20cm (c) 20cm < SSH RMS. Shown are values above (solid) and below (dotted) each depth.

6. Limitations and potential for further work

The statistical estimates which have been shown in this report improve the information provided to the assimilation scheme about the errors in the model and observations. There are a number of limitations in both the method used and the results presented here which should be addressed in future work.

A problem with the method which has been used in this work is that the underlying assumptions are not always valid. As described in section 2, it is assumed that observation errors are uncorrelated but there will be correlations along altimeter tracks which violate this assumption.

This is a general problem with this technique but a way of reducing its effect might be to remove the long wavelength errors from the altimeter data before it is used in the calculation of the statistics, perhaps using a method similar to that described by Le Traon *et al.* (1998). Temperature profile data are also likely to have correlated errors with depth.

The method also relies on there being a large number of observations available for the calculation of the statistics. The number of observations that were available from the three year experiments is shown in section 3. These numbers restricted the amount of information that could be extracted in both spatial and temporal resolution. The finest spatial resolution obtained was 2° in the horizontal and temperature profile statistics were calculated as basin averages to get meaningful results. Statistics also could only be obtained at a limited vertical resolution and only down to 1000m depth. The ideal spatial resolution of these statistics would be on the model grid so that grid scale variations in the variances and correlation scales could be captured by the assimilation scheme although these statistics should be smoothly varying.

One of the choices made in this work was to fit a combination of two SOAR functions to the covariance data. This was done because of the idea that there are two main sources of error in the model and the results generally fitted the covariance data well. Other choices could be made however. If the covariance data could be calculated at finer resolution then more functions could be added to try to extract more components of the error such as some higher baroclinic modes.

The inadequacies in the spatial resolution have already been discussed but there are also benefits to be had by including some temporal resolution. If enough observations were available then it would be possible to obtain statistics which change monthly or seasonally. This would enable any time dependence in the errors to be taken into account when assimilating the data.

It would also be useful to estimate how the errors in the observations are correlated in time so that some estimate is made of how long the observations should be retained in the analyses. If this retention time scale of the observations is accurate then more use can be made of each observation as it can then affect the analysis over the correct period of time.

It would be desirable to produce an improved method for estimating the vertical scales in the temperature profile data for the mesoscale and synoptic scale components. Whilst some progress has been made in understanding how best to project the SSH data onto the subsurface temperature and salinity fields, this is still an unsolved problem and could be worked on further.

No attempt has been made in this work to estimate anisotropic scales in the horizontal, yet it is well known that the correlation scales are anisotropic, especially near the equator where the zonal scales are much larger than the meridional ones. It would also be desirable to produce statistics for salinity data using observations of salinity although this would be difficult at present due to the limited number of these observations available. Some estimates of salinity error variances have been calculated however using the temperature profile statistics together with climatological temperature and salinity fields. The method used and some of the results are described in appendix A. Estimates of the cross-correlations between the different variables would also be useful and would enable a fully multivariate scheme to be used.

A way in which a number of the shortcomings described above could be improved upon would be to use a different, complementary method for estimating the error covariances. The NMC method (Parish, 1992) would provide estimates of the statistics for all model variables on the model grid and would enable estimates of cross-correlations to be made. This would address the

problems of spatial and temporal resolution and might enable more error components to be resolved. The statistics described in this report would not become redundant however as they would be needed to estimate the effects of systematic model error on the statistics when using purely model values. This is because the NMC method does not relate the model forecast to the truth so that systematic errors in the model will distort the resulting statistics. The two methods seem complementary as the method of HL can produce some general large scale estimates of the error statistics and the NMC method can provide the means of producing more detailed spatial and temporal resolution statistics and can also provide estimates of the errors in variables which are not observed, together with cross-correlations between variables. It might also suggest ways of grouping the data to get better results from HL.

This report has concentrated on results of estimating error statistics for the north Atlantic region. However, error statistics are also required over the whole globe so that the global FOAM system can be improved. The results of applying the method to the output of an integration of the 1° resolution global model are briefly described in appendix B.

7. Concluding summary

This report has described some calculations of geographically varying two-component inhomogeneous three-dimensional error covariance statistics for a model of the north Atlantic ocean. This region of the ocean contains areas which are dominated by different dynamical regimes and in which the sources of model forecast errors are also likely to differ. A method has been developed which provides a unified approach to estimating the different types of model error over the whole region, providing estimates of errors which arise from both the internal model dynamics ("mesoscale" errors) and the external forcing of the model ("synoptic" errors). It has been shown that these two sources of model error occur on different scales and so can be clearly separated. The method, based on that of Hollingsworth and Lönnberg (1986), uses collocated model forecast and observation values to form the covariance statistics, and decomposes these into forecast errors on different scales. It also provides a way of estimating the observation errors which include both instrument error and errors of representativity.

A three year (1997-1999) integration of the 1/3° north Atlantic configuration of the Met Office FOAM system was used to form the statistics. The number of observations which were available over this period restricted the resolution at which the statistics could be calculated. For SSH and SST it was possible to produce error variance statistics on a 2° grid whilst statistics for temperature profiles were calculated as basin averages. At the surface the results show that mesoscale error variances dominate in the Gulf Stream region and synoptic scale errors become more important elsewhere. The average mesoscale variances decrease with depth so that they are of similar size to the synoptic variances at 1200m depth. Spatially varying correlation scales were also calculated at the surface which showed that the average mesoscale error length scales were about 40-60km whereas those for synoptic scale errors were about 400-500km. The synoptic correlation scales increase below the surface to a maximum of about 1000km at 100m depth whereas the mesoscale length scales remain fairly constant with depth.

Vertical correlation scales for the two error components were estimated using temperature profile data. The synoptic scale vertical correlation estimates gave reasonable results whereas the mesoscale vertical correlation scales seemed quite incoherent and were also smaller than expected. More work is needed to produce better estimates of these quantities. A method was used to test how well the Cooper & Haines scheme represents the lifting and lowering implied by the observations. This also used the temperature profile data and showed that more

lifting/lowering of model profiles should be carried out in the region of the thermocline and less above and below.

The main limitations of the Hollingsworth and Lönnberg (1986) method to calculate error statistics are that it assumes that observational errors are uncorrelated and the spatial and temporal resolution at which the statistics can be estimated depends on the number of observations and is very limited for ocean profile data. Also, statistics can only be estimated for variables which are observed. The main advantage of the method is that the observations used in the calculations provide a connection with the "true" ocean.

References

Argo Science Team (1998). On the design and implementation of Argo – an initial plan for a global array of profiling floats. *TCPO Report No. 21, GODAE Report No. 5.* Published by the GODAE International Project Office, BMRC, Melbourne, Australia, 32 pp.

Bell, M.J., R.M. Forbes, and A. Hines, 2000. Assessment of the FOAM global data assimilation system for real-time operational ocean forecasting, *J. Mar. Syst.*, 24, 249-275.

Cooper, M. and K. Haines, 1996. Altimetric assimilation with water property conservation, *J. Geophys. Res.*, **101**, 1059-1077.

Cox, M.D., 1984. A primitive equation, 3-dimensional model of the ocean, *GFDL Ocean GroupTech. Rep. No. 1*, Geophysical Fluid Dynamics Laboratory, 143.

Daley, 1991. *Atmospheric Data Analysis*, Cambridge University Press.

Evensen, G., 1997. Advanced data assimilation for strongly nonlinear dynamics, *Mon. Wea. Rev.*, 125, 1342-1354.

Faucher, P., M. Gavart and P. De Mey, 2002. Isopycnal empirical orthogonal functions (EOFs) in the north and tropical Atlantic and their use in estimation problems. *J. Geophys. Res.*, **107**, 21-1 to 21-17.

Global Ocean Data Assimilation Experiment, 2002. En route to GODAE, proceedings of the international symposium, 13-15th June, 2002, Biarritz, France.

Gavart, M. and P. De Mey, 1997. Isopycnal EOFs in the Azores Current region: a statistical tool for dynamical analysis and data assimilation, *J. Phys. Oceanogr.*, **27**, 2146-2157.

Gordon, C., C. Cooper, C., C. A. Senior, H. Banks, J. M. Gregory, T. C. Johns, J. F. B. Mitchell and R. A. Wood, 2000. The simulation of SST, sea ice extents and ocean heat transports in a version of the Hadley Centre coupled model without flux adjustments, *Climate Dyn.*, 16, 147-168.

Hollingsworth, A. and P. Lönnberg, 1986. The statistical structure of short-range forecast errors as determined from radiosonde data. Part I: The wind field., *Tellus*, **38A**, 111-136.

Jacobs, G.A., C.N. Barron and R.C. Rhodes, 2001. Mesoscale characteristics, *J. Geophys. Res.*, **106**, 19,581-19,595.

Le Traon, P.Y., F. Nadal and N. Ducet, 1998. An improved mapping method of multisatellite altimeter data, *J. Atmos. Oceanic Technol.*, **15**, 522-534.

Levitus, S., R. Burgett and T. Boyer, 1994. World ocean atlas 1994. Volume 3: Salinity and Volume 4: Temperature. *NOAA Atlas NESDIS 3 & 4.*

Lorenc, A.C., 1986. Analysis methods for numerical weather prediction, *Quart. J. R. Met. Soc.*, 112, 1177-1194.

Lorenc, A.C., R.S. Bell and B. MacPherson,1991. The Met Office analysis correction data assimilation scheme, *Quart. J. R. Met. Soc.*, **117**, 59-89.

Parish, D.E. and J.C. Derber, 1992. The National Meteorological Center's spectral statistical-intepolation analysis system, *Mon. Wea. Rev.*, **120**, 1747-1763.

Weber, R.O. and P. Talkner, 1993. Some remarks on spatial correlation function models, *Mon. Wea. Rev.*, **121**, 2611-2617.

Xu, Q. and L. Wei, 2001. Estimation of three-dimensional error covariances. Part I: Analysis of height innovation vectors. *Mon. Wea. Rev.*, **129**, 2126-2135.

Appendix A

Estimating salinity statistics for the north Atlantic and Arctic

The number of salinity observations available for assimilation into the FOAM system before 1998 was very small. The number of these observations is set to increase substantially with the implementation of the Argo project (Argo Science Team, 1998), for example, 431 Argo floats reported salinity in October 2002. Appropriate assimilation of these data into the FOAM system should therefore bring about a marked improvement in the salinity field. This requires some estimate of the error covariance statistics for salinity.

The experiment described in section 3 which provided the data for the calculations of error statistics did not assimilate salinity data. It is therefore not possible to calculate error statistics for the salinity data directly from the model output as was done for the other data types. Instead, a method is used which estimates these statistics using the temperature profile statistics together with climatological temperature and salinity values.

To estimate the error variances for salinity from those calculated using temperature data, the two are assumed to be related through the following equation,

$$< (S_i^f - S_i^t)^2 >= \alpha_i^2 < (T_i^f - T_i^t)^2 >, \qquad \text{(A.1)}$$

where α_i represents some time-average value of the ratio of the salinity variations to the temperature variations at point i, and is given by

$$\alpha_i = < dS_i > / < dT_i > . \qquad \text{(A.2)}$$

The climatological temperature and salinity data of Levitus *et al.* (1994) was used to provide estimates of α_i. This was done by splitting the model domain into 10° resolution grid boxes and calculating the interquartile range of temperature and salinity values in each box and at each depth over the year. This gives an estimate of the range of values which are expected in each grid box for each variable. The field of values of these ratios is then used to give some estimate of the error variance for salinity by using (A.1) above. Figures A1(a) and (b) show examples of α_i for the north Atlantic at the surface and at 300m depth. Examples of the mesoscale error variance for salinity are shown in figures A2(a) and (b) for the surface and 300m depth respectively.

Estimates of the error correlation scales for salinity cannot be estimated in the same way. Until more data is available for salinity, these will be set to the same values as for the temperature data.

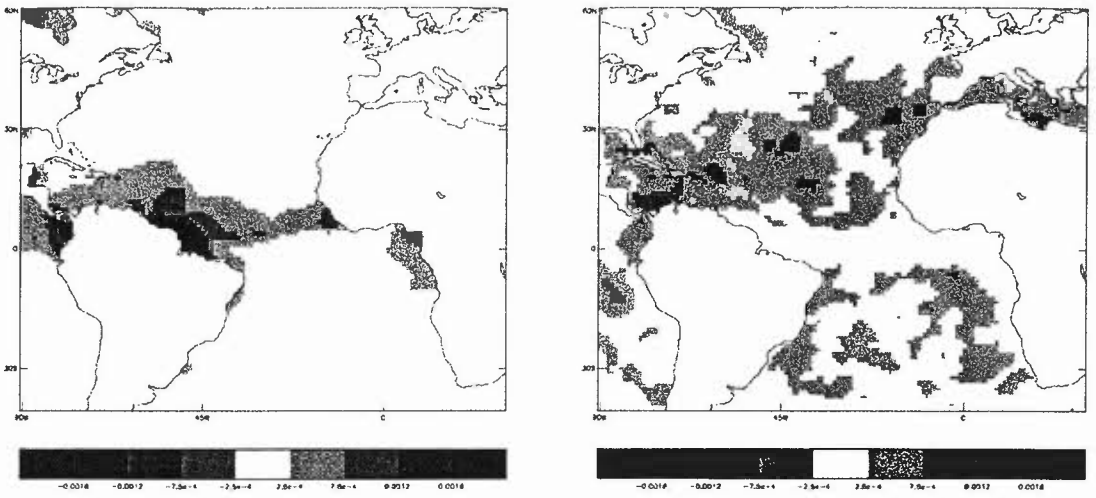

Figure A1: α_l (psu K^{-1}) at (a) the surface and (b) 300m depth.

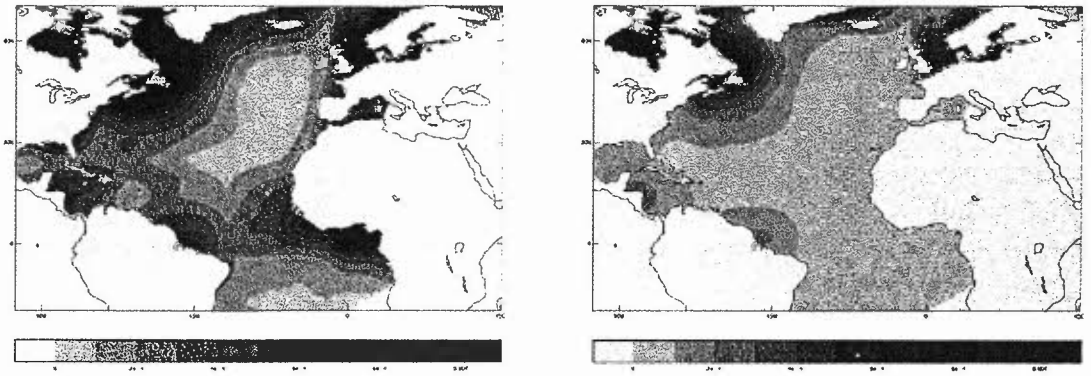

Figure A2: Salinity mesoscale error variances (psu^2) at (a) the surface and (b) 300m depth.

Appendix B

Estimates of global error covariance statistics

This appendix gives a summary of the results of estimating error covariance statistics for the entire global ocean. The data used in these calculations were obtained from a 3 year integration of the 1° resolution global FOAM system which ran between 1997 and 1999 assimilating SST and temperature profile data. Collocated observation and model forecast values were output from this integration. The same method as described in section 2 was used to calculate the statistics. Only SST statistics are shown here.

Some regions of the globe contained few observations, particularly at high latitudes in both hemispheres. In these areas, the estimates of variances and correlation scales were not statistically significant and so the values have been extrapolated/interpolated from regions where a good estimate has been found.

The variances for SST are shown in figures B1(a) and (b) for the mesoscale and synoptic scale components respectively. In contrast to the results for the 1/3° resolution north Atlantic model, the synoptic scale error variances are inhomogeneous and are of similar amplitude to the

mesoscale variances. The regions of high error variance are similar for both the mesoscale and synoptic scales. These generally occur in the areas of the major ocean currents. For instance, the Gulf Stream has the highest error variance closely followed by the Kurushio current. The mesoscale error variances are also large in the Agulhas current region, the southern Indian ocean, the eastern Australian current, the region to the northeast of Drakes passage and in the region off the coast of Peru.

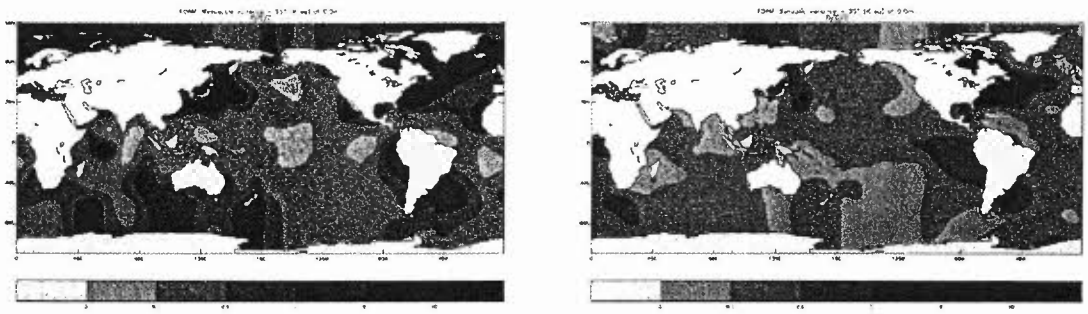

Figure B1: SST forecast error variance (K^2) (a) mesoscale and (b) synoptic scale.

Figures B2(a) and (b) show the error correlation scales for the mesoscale and synoptic scales respectively. These figures show that the split between the two error components is not always as clearly defined as it was in the 1/3° resolution model of the north Atlantic. For instance, there are regions, particularly in the southern Pacific and Atlantic oceans where the mesoscale correlation scales are as large as 200km which is much larger than the Rossby radius and is of a similar order to the synoptic scale correlation scales. Elsewhere, there does appear to be a well-defined split between the two components.

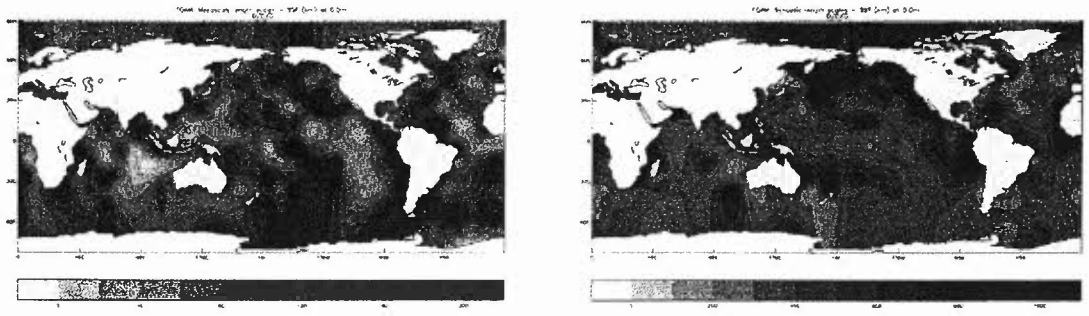

Figure B2: SST forecast error correlation scales (km) (a) mesoscale and (b) synoptic scale.

The observation error variances are shown in figure B3. The maximum values are smaller than either the mesoscale or synoptic scale error variances and occur mainly at mid-latitudes in both hemispheres. There are also some larger values in the eastern tropical Pacific.

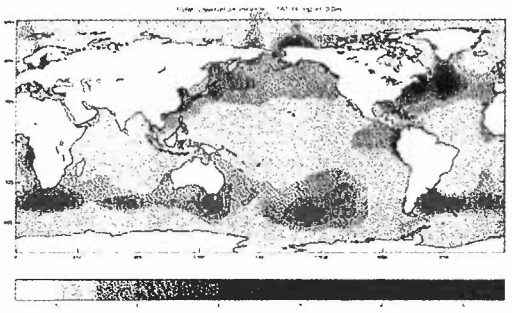

Figure B3: SST observation error variance (K^2).

The way these statistics should be used in a model with a resolution of 1° in the horizontal is different than for an eddy resolving or eddy permitting model. This is because the mesoscale correlation length scales are generally significantly smaller then the model grid so that observation increments will not be spread out into the model field. This means that point values will be put into the model field in the assimilation which could have adverse impacts on the subsequent model forecast. Because the mesoscale length scales are smaller than the model grid spacing, they should be counted as errors of representativity and included in the observation errors.